Submitted to

**32nd International Conference on High Energy Physics, ICHEP04**, August 16, 2004, Beijing
Abstract: **6-0180**
Parallel Session **6**

*www-h1.desy.de/h1/www/publications/conf/conf_list.html*

# Elastic Photoproduction of $J/\psi$ Mesons at HERA

H1 Collaboration

**Abstract**

The elastic $J/\psi$ photoproduction cross section $\sigma(\gamma p \rightarrow J/\psi p)$ is measured in the kinematic region $Q^2 < 1\ \mathrm{GeV}^2$, $40\ \mathrm{GeV} < W_{\gamma p} < 150\ \mathrm{GeV}$ and $|t| < 1.2\ \mathrm{GeV}^2$ using the muon decay channel. The analysis is based on an integrated luminosity of $\mathcal{L} = 54.8\ \mathrm{pb}^{-1}$. Single and double differential cross sections are measured as a function of $W_{\gamma p}$ and $|t|$ and are compared to calculations in perturbative QCD.

# Introduction

Elastic photoproduction of $J/\psi$ mesons has been studied previously by the H1 and ZEUS experiments at HERA [1, 2]. Here, we report on a new measurement with increased statistics, which allows a study of the dependence of the elastic photoproduction cross section as a function of $W_{\gamma p}$ , the photon proton centre-of-mass energy, and of $|t|$, the squared four-momentum transfer at the proton vertex, with increased precision. The $W_{\gamma p}$ and $|t|$ dependences of the cross section are analysed single and double-differentially.

The preliminary results are compared to calculations in perturbative Quantum Chromodynamics, where the process of diffractive charmonium production in $\gamma p$ scattering is described as follows. An almost real photon, emitted from the incoming lepton, fluctuates into a $c\bar{c}$ pair. The $c\bar{c}$ pair subsequently interacts with the proton via the exchange of two gluons (or a gluonic ladder) in a colour-singlet state and then evolves into a $J/\psi$ meson.

# Data Analysis

For this analysis, data collected with the H1 detector in the years 1999 and 2000 are used. During this period, HERA collided $27.6$ GeV positrons[1] with $920$ GeV protons, with an integrated luminosity of $\mathcal{L} = 54.8\ \mathrm{pb}^{-1}$ are used. The data selection is very similar to previous H1 analyses [1,3]. Photoproduction events are selected by rejecting events with electromagnetic energy clusters above $8$ GeV in the Liquid Argon or the Spacal calorimeters. This restricts the photon virtuality to $Q^2 < 1\ \mathrm{GeV}^2$. $J/\psi$ mesons are reconstructed via their leptonic decay into muons. The data selection requires exactly two oppositely charged tracks in the central region[2] $20^\circ \leq \theta \leq 160^\circ$, at least one of which is identified as a muon either as a minimally ionising particle in the liquid argon calorimeter or as a highly penetrating particle reaching the instrumented iron surrounding the calorimetry.

In elastic photoproduction of $J/\psi$ mesons, both the scattered positron and the scattered proton are not generally detected. The largest contribution to the background is events in which the proton dissociates. Most of the events with proton dissociation are rejected by demanding no deposits in the forward section of the calorimeter ($\theta < 10^\circ$), the proton remnant tagger ($0.06^\circ < \theta < 0.26^\circ$) and the forward muon detector ($3^\circ < \theta < 17^\circ$).

The resulting mass distribution of the the muon pairs is shown in fig.1 for the range $40\ \mathrm{GeV} < W_{\gamma p} < 150\ \mathrm{GeV}$ and $|t| < 1.2\ \mathrm{GeV}^2$. The remaining non-resonant back-

[1] For the first half of the year 1999, HERA collided $27.6$ GeV electrons with $920$ GeV protons. Since this measurement is not sensitive to the incoming lepton charge, the term 'positrons' will be used for both electrons and positrons.

[2] The coordinate system of H1 defines the positive $z$ axis to be in the direction of the outgoing proton beam. The polar angle $\theta$ is the defined with respect to the positive $z$ axis.

ground is dominated by the process $\gamma\gamma \to \mu^+\mu^-$, where one of the photons originates from the beam positron and the other from the beam proton. The number of $J/\psi$ signal events is obtained for each analysis bin by fitting the invariant mass distribution with the sum of a Gaussian and a power law distribution to parameterise the background.[3] The systematic error on the fits is obtained by varying the function used to describe the background and also by counting all events within a mass window of $2.9$ GeV $< M_{\mu^+\mu^-} < 3.3$ GeV and subtracting the fitted background.

The resulting number of signal events is corrected for detector acceptance, efficiency losses and remaining background from proton dissociation using the Monte Carlo program DIFFVM [4]. It can be used to generate both elastic and proton dissociative processes. The correction for proton dissociation has been checked with the data and is typically 15%.

The efficiency for muon identification and of the triggers are checked and adjusted to data where necessary using independent data samples. The remaining differences between data and MC contribute to the systematic error. The total systematic error is estimated to be 12%. The dominant error sources are the determination of the proton dissociative background (5-10%) and the trigger efficiencies (6%).

# Results

After correcting the observed number of events in each bin for detector acceptance and efficiencies, the $ep$ cross section is obtained. It is converted into a $\gamma p$ cross section assuming factorisation of the $ep$ reaction into emission of photons described by a photon flux and the $\gamma p$ interaction. The cross section for the full range $|t| < 1.2$ GeV$^2$ is presented in fig.2 as a function of $W_{\gamma p}$ .

A combined fit of the form $\sigma \propto W_{\gamma p}^{\delta}$ is performed using separate normalisation factors for this data set and the $J/\psi \to e^+e^-$ data points[4] [1] also shown in the figure. The fit yields a value[5] of $\delta = 0.70 \pm 0.08$, which is in agreement with previous measurements [1] and the latest results from the ZEUS collaboration [2]. In fig.3 the same data are shown, this time in comparison with results from the ZEUS collaboration and QCD based theoretical calculations [6–9], which describe the steep rise of the cross section qualitatively.

The fit to the $W_{\gamma p}$ dependence is repeated for bins of $|t|$, which yields an effective pomeron trajectory via $\delta = 4 \cdot (\alpha_{\mathbb{P}}(t) - 1)$. The results for $\alpha_{\mathbb{P}}(t)$ are shown in fig.4 and compared with ZEUS data [2]. A linear effective trajectory ($\alpha_{\mathbb{P}}(t) = \alpha_0 + \alpha'_{\mathbb{P}} \cdot t$ GeV$^{-2}$) is assumed and fitted yielding $\alpha_{\mathbb{P}}(t) = (1.20 \pm 0.02) + (0.15 \pm 0.06) \cdot t$ GeV$^{-2}$. The effect of shrinkage is observed with a significance of three standard deviations.

[3] A second Gaussian distribution is used for the $\psi'$ signal.

[4] A correction ranging from +10% to +14% was applied to the six data points above $W_{\gamma p} > 135$ GeV as compared to [1]. In [1] the branching ratio for $J/\psi \to e^+e^-\gamma$ [5] was erroneously assumed not to be included in that for $J/\psi \to e^+e^-$.

[5] The statistical and systematic errors are added in quadrature.

In fig.5 the dependence of the photoproduction cross section of $J/\psi$ mesons as a function of $|t|$ is studied in the region of $40\ \mathrm{GeV} < W_{\gamma p} < 150\ \mathrm{GeV}$. This dependence is measured averaging over the entire $W_{\gamma p}$ range. Assuming an exponential behaviour $e^{-b|t|}$, a fit yields an elastic slope parameter $b = 4.65 \pm 0.08$. The procedure is repeated in bins of $W_{\gamma p}$ and the resulting $b$ values are shown in fig.6. Here a fit of the form $b(W_{\gamma p}) = b_0 + 4\alpha' \cdot \ln(W_{\gamma p}/90\ \mathrm{GeV})$ has been performed, yielding $b_0 = (4.73 \pm 0.12)\ \mathrm{GeV}^{-2}$ and $\alpha' = (0.19 \pm 0.08)\ \mathrm{GeV}^{-2}$. Both parameters are in good agreement with those derived from the fits in fig.4 and 5.

# Acknowledgments

We are grateful to the HERA machine group whose outstanding efforts have made this experiment possible. We thank the engineers and technicians for their work in constructing and now maintaining the H1 detector, our funding agencies for financial support, the DESY technical staff for continual assistance and the DESY directorate for support and for the hospitality which they extend to the non DESY members of the collaboration.

# References

[1] H1, C. Adloff *et al.*, Phys. Lett. **B483**, 23 (2000), hep-ex/0003020.

[2] ZEUS, S. Chekanov *et al.*, Eur. Phys. J. **C24**, 345 (2002), hep-ex/0201043.

[3] D. Schmidt, *Diffraktive Photoproduktion von Charmonium im H1 Detektor bei HERA*, PhD thesis, University of Hamburg, 2001.

[4] B. List and A. Mastroberardino, in *Proc. of the Workshop on Monte Carlo Generators for HERA Physics*, p. 396, 1999, DESY-PROC-1999-02.

[5] Particle Data Group, C. Caso *et al.*, Eur. Phys. J. **C3**, 1 (1998).

[6] H. L. Lai *et al.*, Phys. Rev. **D55**, 1280 (1997), hep-ph/9606399.

[7] A. D. Martin, R. G. Roberts, W. J. Stirling, and R. S. Thorne, Eur. Phys. J. **C4**, 463 (1998), hep-ph/9803445.

[8] CTEQ, H. L. Lai *et al.*, Eur. Phys. J. **C12**, 375 (2000), hep-ph/9903282.

[9] A. C. Caldwell and M. S. Soares, Nucl. Phys. **A696**, 125 (2001), hep-ph/0101085.

[10] M. Binkley *et al.*, Phys. Rev. Lett. **48**, 73 (1982).

[11] B. H. Denby *et al.*, Phys. Rev. Lett. **52**, 795 (1984).

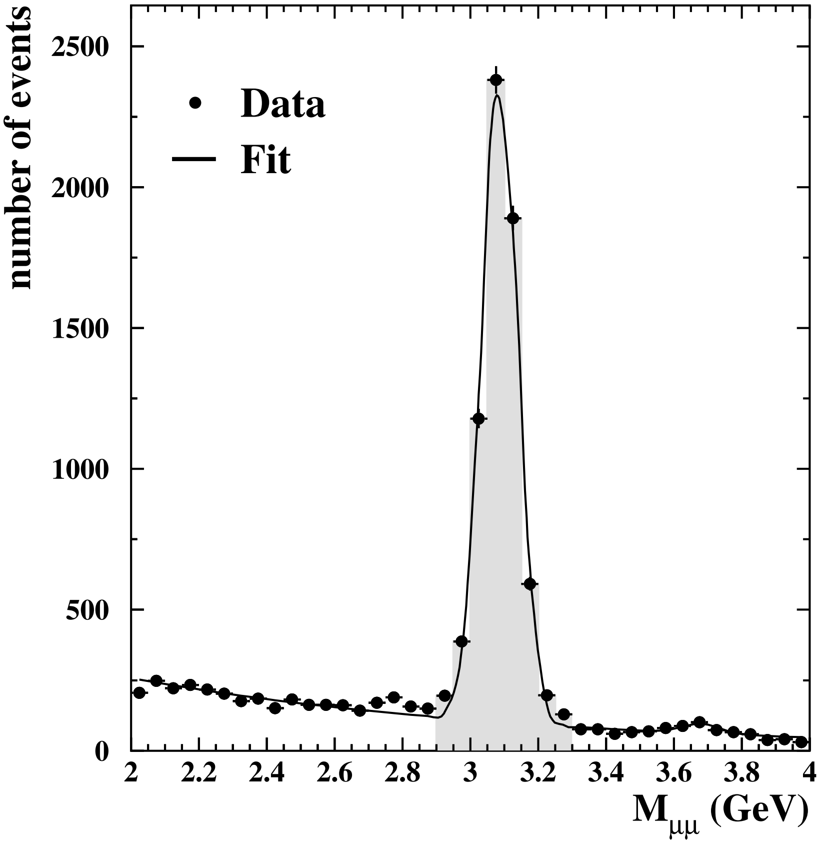


**Figure 1:** The dimuon mass spectrum after final data selection. The curve shows the result of a fit combining two Gaussian distributions for the $J/\psi$ and $\psi'$ signals and a power law parametrisation of the non-resonant background. The number of events in the signal are extracted in a mass window between 2.9 GeV and 3.3 GeV.

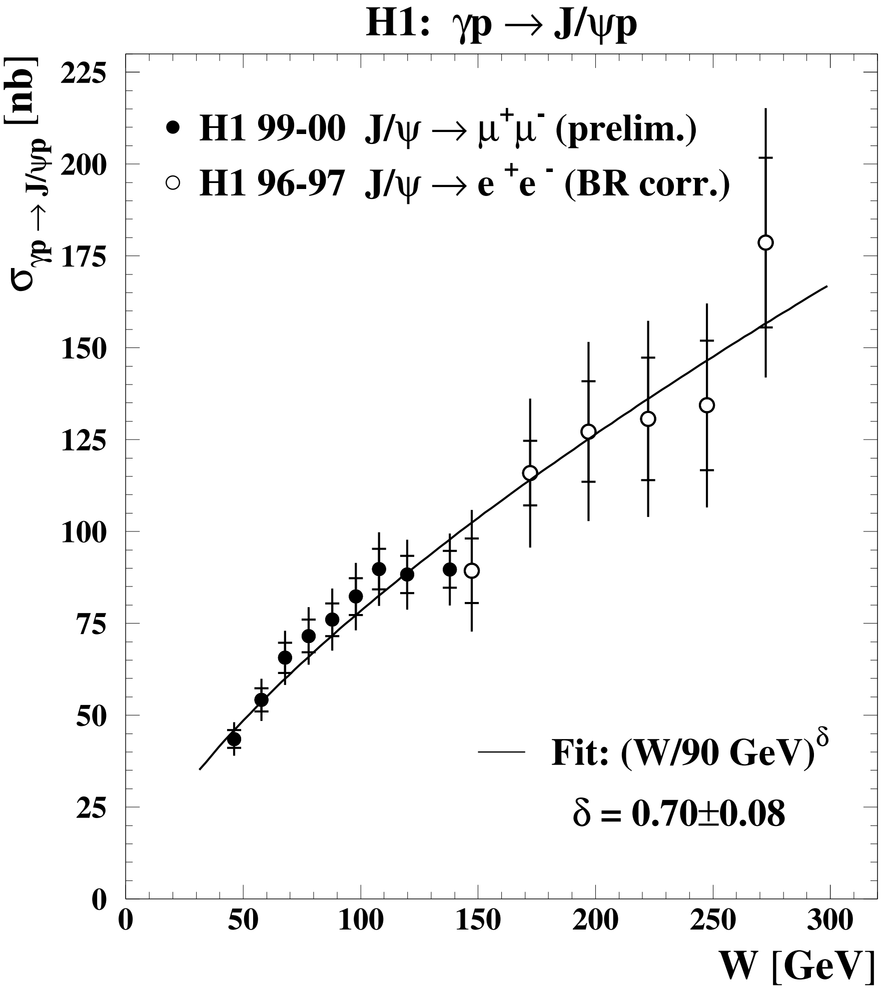


**Figure 2:** The elastic cross section $\sigma_{\gamma p}$ as a function of $W_{\gamma p}$ . The inner (outer) bars give the statistical (total) error. The data from the process $J/\psi \to e^+e^-$ are from [1]. The fit is applied to the two data sets, allowing different normalisation factors for both.

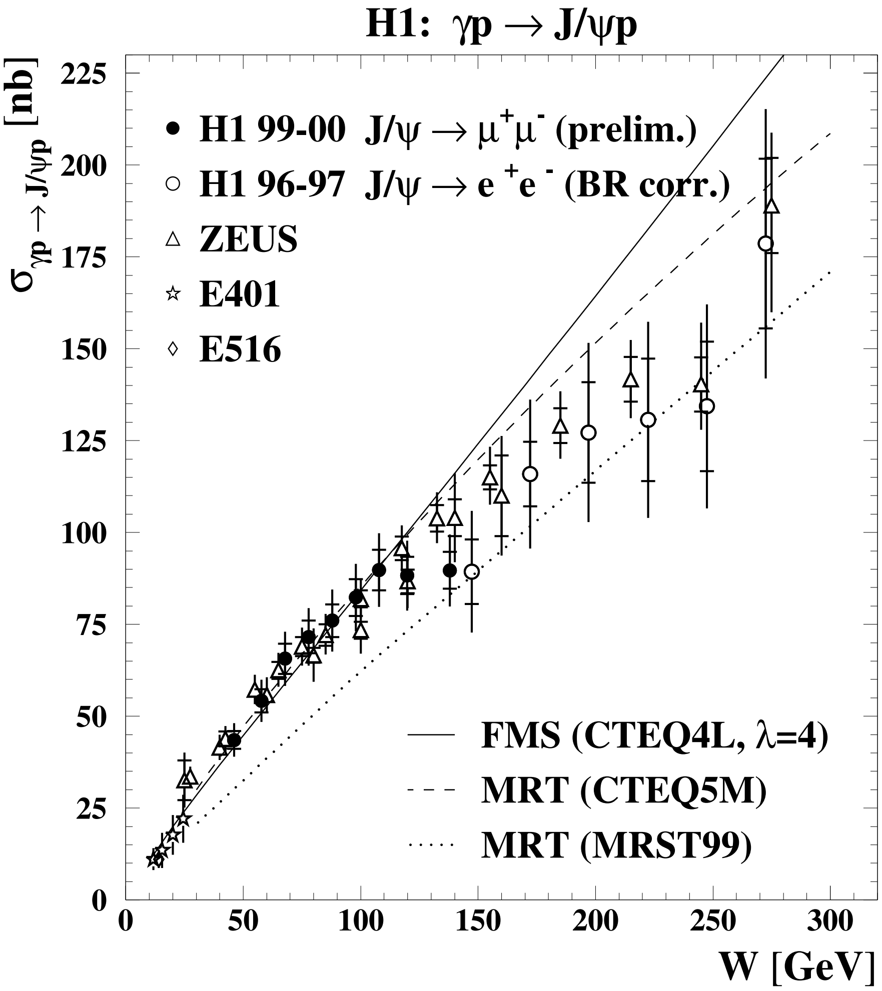


**Figure 3:** The elastic cross section $\sigma_{\gamma p}$ as a function of $W_{\gamma p}$ . The inner (outer) bars give the statistical (total) error. The experimental data [2, 10, 11] are compared with pQCD models [6–9].

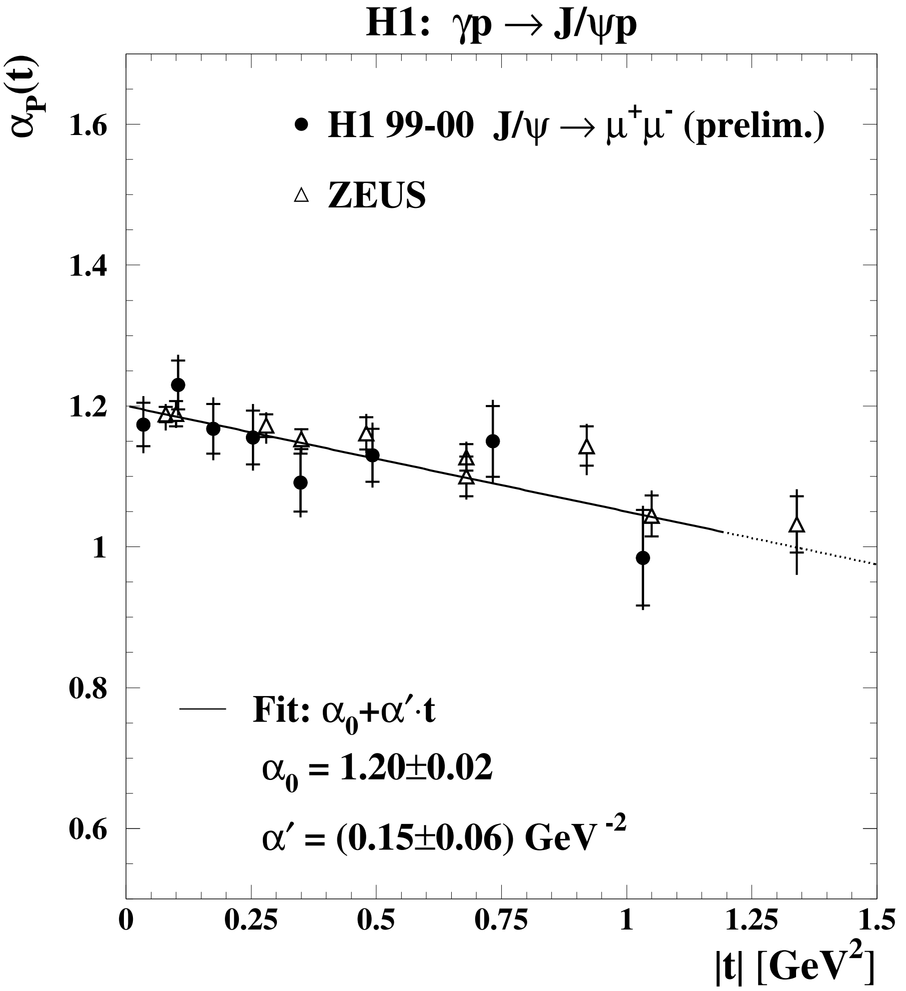


**Figure 4:** The effective pomeron trajectory as a function of $|t|$. The inner (outer) bars give the statistical (total) error. A linear form is assumed and fitted to the H1 data. The ZEUS data are from [2]. Shrinkage is observed with a significance of three standard deviations.

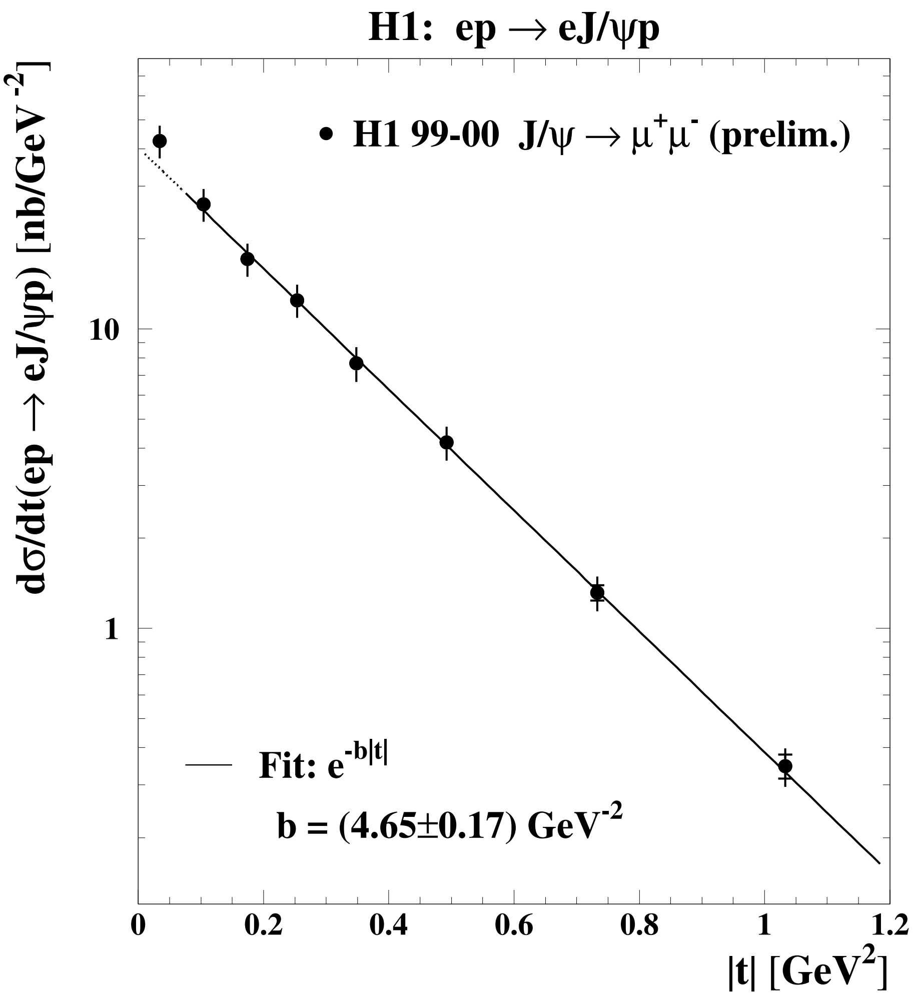


**Figure 5:** The differential cross section $d\sigma/dt$ as a function of $|t|$. The inner (outer) bars give the statistical (total) error. The result of a fit of the form $d\sigma/dt \propto e^{bt}$ in the range $0.07\ \mathrm{GeV}^2 < |t| < 1.2\ \mathrm{GeV}^2$ is shown as the solid line.

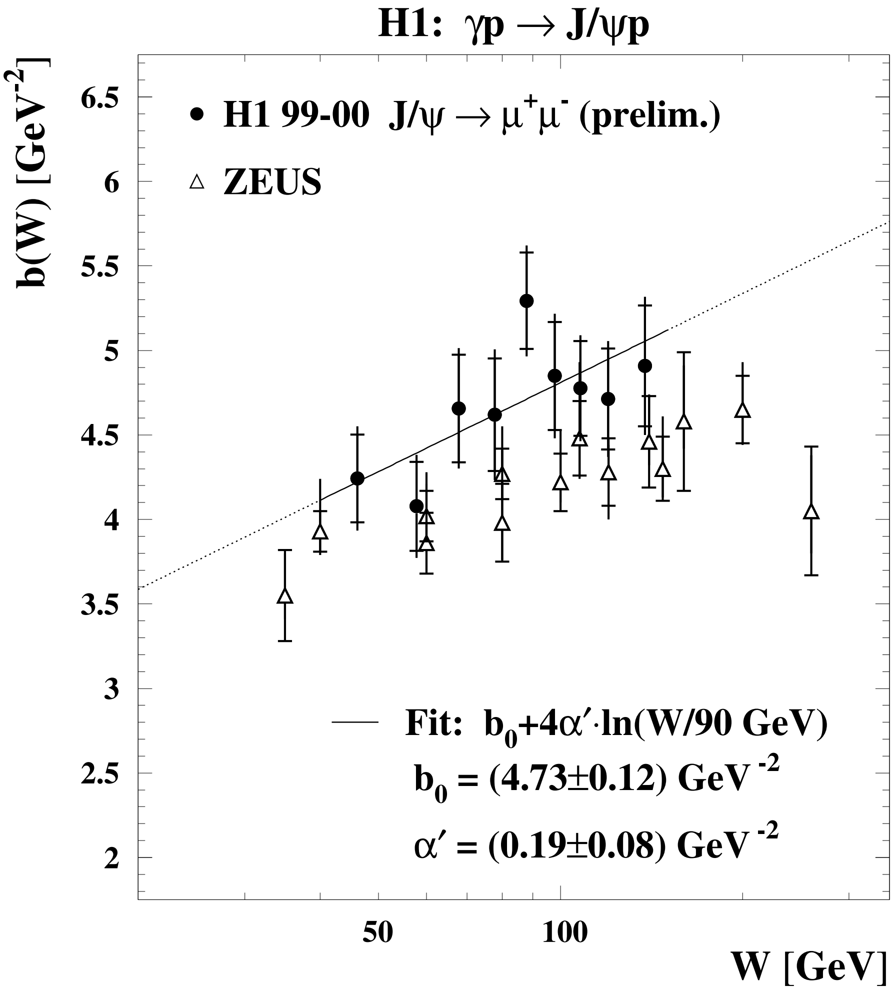


**Figure 6:** The slope parameter $b$ derived from a fit to the differential cross section $d\sigma/dt \propto e^{bt}$ as a function of $W_{\gamma p}$ together with the ZEUS data [2]. The inner (outer) bars give the statistical (total) error. The result of a fit of the form $b(W_{\gamma p}) = b_0 + 4\alpha' \cdot \ln(W_{\gamma p}/90 \text{ GeV})$ in the range $40 \text{ GeV} < W_{\gamma p} < 150 \text{ GeV}$ is shown as the solid line.